Ceramics International xxx (xxxx) xxx

Contents lists available at ScienceDirect

Ceramics International

journal homepage: www.elsevier.com/locate/ceramint

Electrical characterization of glass-ceramic sealant-metallic interconnect joined samples under solid oxide electrolysis cell conditions; influence on the microstructure and composition at the different polarized interfaces

Hassan Javed [a,*], Kai Herbrig [a], Antonio Gianfranco Sabato [b], Domenico Ferrero [c], Massimo Santarelli [c], Christian Walter [a], Federico Smeacetto [d]

[a] Sunfire GmbH, Gasanstaltstraße 2, 01237, Dresden, Germany
[b] IREC-Institut de Recerca en Energia de Catalunya, 08930, Sant Adrià de Besòs Barcelona, Spain
[c] Department of Energy (DENERG), Politecnico di Torino, 10129, Turin, Italy
[d] Department of Applied Science and Technology (DISAT), Politecnico di Torino, 10129, Turin, Italy

ARTICLE INFO

Keywords:
Solid oxide cell
Sealants
Glass-ceramic
Electrical resistivity

ABSTRACT

In this study, the electrical resistivity of a glass-ceramic sealant is evaluated at 850 °C, for 2800 h under the applied voltage of 1.6 V. The glass-ceramic sealant is sandwiched between two Crofer22APU plates to produce Crofer22APU/Glass-ceramic/Crofer22APU samples. The Crofer22APU/glass-ceramic/Crofer22APU joints show electrical resistivity around 10^6-10^7 Ω cm, significantly high to ensure the insulation between two conductive interconnect plates. The detailed SEM-EDS post mortem analysis showed good thermo-mechanical compatibility of the glass-ceramic with the Crofer22APU substrates, thus excluding any detrimental interaction with the metallic interconnect under high applied voltage. XRD analysis of glass-ceramic confirmed the presence of crystalline phases with suitable CTEs, after electrical resistivity under harsh conditions.

1. Introduction

Hydrogen is considered as one of the most promising energy sources and as an alternative to fossil fuels. In this context, solid oxide electrolysis cell (SOEC) technology has attained special attention to generate pure hydrogen from direct electrolysis of water, thanks to its higher efficiency compared to low-temperature electrolysis technologies [1–5]. A SOEC stack consists of different repeating units, each consisting of a cell composed of two electrodes and electrolyte, stacked above each other by a metallic interconnect that ensures fluids distribution and electrical connection between adjacent cells. In the planar configuration of a SOEC stack, the role of sealants is fundamental as they have to minimize the gas leakage or mixing at either electrode and to provide electrical insulation between two adjacent metallic interconnects [6–8].

SOECs are usually operated in the range of 750–900 °C. For such a high operating temperature and an expected working life of >40,000 h, the selection of SOEC stack components is quite challenging [9–11]. In particular, the sealants for a SOEC stack should be chemically, mechanically and thermally stable under harsh working conditions [12]. Glass-ceramics are considered as the most efficient sealing materials due to their higher mechanical and thermal stability at high temperature, high electrical resistivity and low production cost [13–18].

The reactivity between the glass-ceramic sealing (specifically when considering the residual glassy phase) and the metallic interconnect has to be as low as possible, in order to limit the degradation at the interface thus affecting the adhesion and thermomechanical properties.

To date several glass-ceramic sealants have been synthesized and studied for solid oxide fuel cell (SOFC) applications [7,19–24]. In SOEC, the sealants face similar working conditions as that of SOFC; however, they are subjected to a higher applied voltage during the electrolysis mode [25]. For this reason, the investigation of the effects of an applied electrical load can be even more challenging in the case of SOEC application, especially considering the harsh working environment.

The glass-ceramics have generally high electrical resistivity; however, the chemical interaction of glass with metallic interconnect can form conducting phases and consequently can result in short circuit [26], or in general reduces the electric resistivity of the sealant. In some cases, these reactions have an electrochemical nature and may be triggered by the application of an electrical voltage of a certain magnitude. A number of studies have investigated the electrical behaviour of

* Corresponding author.
E-mail address: hassan.javed@sunfire.de (H. Javed).

https://doi.org/10.1016/j.ceramint.2020.11.176
Received 24 October 2020; Received in revised form 21 November 2020; Accepted 21 November 2020
Available online 25 November 2020

glass-ceramic sealants for SOFC applications [27–32]. For instance, Ghosh et al. [33] measured the electrical resistivity of different glass-ceramic systems at 800 °C in air. The glass-ceramics showed resistivity in the range of 10^4-10^6 Ω cm as measured up to 100 h. In another study, Chou et al. [29] observed a stable electrical resistivity of 10^4-10^6 Ω cm of different glass systems as measured up to 800 h at 850 °C and 0.7 V. However, post-mortem analysis showed presence of chromates and consequently cracks within the glass-ceramic sealants. The existing literature on glass-ceramic sealant is extensive and focuses particularly on thermal and thermo-mechanical properties. There is a relatively small body of literature that is concerned with electrical resistivity of sealants-interconnects in harsh conditions. Rost et al. [31] investigated the electrical resistivity of different glass-ceramic systems sandwiched between two Crofer22APU plates, under the applied voltages ranging from 0.7 V to 30 V, in dual atmosphere. Most of the studied sealants showed big pores after only 200–300 h of resistivity test at 30 V. However, the paper discussed the analysis only up to 500 h. Sabato et al. [32] investigated the effects of two different DC voltage values (0.7 V and 1.3 V) to an alkali containing glass-ceramic at 800 °C exposed to dual atmosphere. In the case of lower applied voltage, the resistivity of the samples remained almost constant at 10^5 Ω cm during the 100 h test. On the contrary, the application of 1.3 V lead to a continuous decreasing in the resistivity as an indication of the development of detrimental reaction between the alkali metal oxide contained in the sealant and Crofer22APU stainless steel. There is evidence that voltage plays a crucial role in affecting sealant's performance.

In the present work, the electrical resistivity of the Crofer22APU/glass–ceramic/Crofer22APU joined samples was studied by using a SrO-containing glass-based system (further labelled as HJ4), specifically designed for a working temperature of 850 °C under SOEC conditions. According to previously performed studies, the HJ4 glass–ceramic has CTE of 9.3×10^{-6} K^{-1} that is closely matching CTE of the Crofer22APU. High temperature mechanical characterization confirmed that HJ4 glass-ceramic is suitable for SOEC application 850 °C. The XRD analysis showed the presence $SrSiO_3$ and SiO_2 phases after the joining [14,34]. Sr based glass-ceramic compositions often results in the formation of low CTE celsian phase ($SrAl_2Si_2O_8$), having a CTE of 2.7×10^{-6} K^{-1} [23,35], however, HJ4 glass-ceramic is free from celsian phase.

The joined samples were tested up to 2800 h with the application of a constant DC voltage of 1.6 V. The resistivity was measured during all the duration of the test. The SEM-EDS post mortem analyses were carried out to investigate the microstructure of glass-ceramic sealants and the compatibility with the Crofer22APU interconnect.

2. Experimental

Crofer22APU/glass-ceramic/Crofer22APU joined samples were prepared for the electrical characterization. Prior to joining, the Crofer22APU (from VDM® Metals) plates having dimension of 3 × 3 cm^2 were cleaned by sonication in order to remove any contamination. The glass was deposited on a Crofer22APU substrate in the form of slurry composed of glass particles and ethanol. The joining was processed at 950 °C for 5 h at a heating rate of 2 °C/min. Further details about the joining parameters can be found in our previous studies [14,34].

In order to measure the electrical resistivity of Crofer22APU/glass-ceramic/Crofer22APU joint at high temperature with an applied voltage between the plates, the sample was put in a muffle furnace (FALC, Treviglio, Italy) on an alumina base and connected to a voltage generator and a measuring circuit by platinum wires point welded on each plate (Fig. 1). A voltage of 1.6 V was applied and test temperature of 850 °C that was maintained during the test. Samples were exposed to static air during the whole test.

The resistivity of the joint was indirectly evaluated by measuring the voltage drop – V_m – on a known resistance R_m in series with the sample and solving the circuit to calculate the resistance of the sample R_S. The resistivity was evaluated from the resistance of the joint sample and the geometry (area and thickness) of the sealing. The voltage drop was measured every second using a self-developed acquisition system based on CompactDAQ hardware and LabVIEW Signal Express software (National Instruments, Austin, USA).

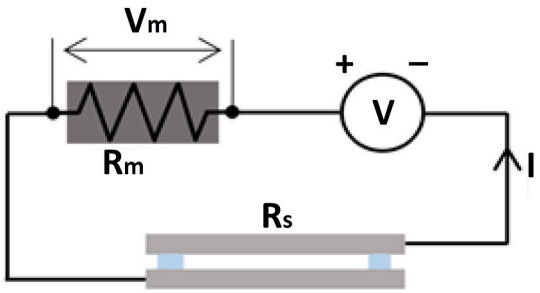

Fig. 1. Schematic of the measuring setup for electrical resistivity. The joint sample R_S is connected in series to a voltage generator V and a measuring resistance R_m.

After the electrical resistivity analysis, the Crofer22APU/glass-ceramic/Crofer22APU samples were investigated under scanning electron microscope (SEM, Merlin ZEISS, Munich, Germany). For this purpose, cross sections of the samples were polished up to 1 μm by diamond paste and investigated by SEM after being coated with gold. The crystalline phases in the glass-ceramic after the electrical resistivity test were analysed by using X-ray diffraction (XRD); PanAlytical X'Pert Pro PW 3040/60 Philips (the Netherlands), with Cu Kα and the X'Pert software. The XRD analysis were carried out in the range of 2 theta 10°–70°, with step size of 0.02626° and time per step 10.20 s.

3. Results and discussion

3.1. Electrical resistivity analysis

Fig. 2 shows the electrical resistivity data of the HJ4 glass-ceramic sandwiched between two Crofer22APU plates. Fig. 2 depicts that the resistivity is in the range of (10^6-10^7 Ω cm) as measured at 850 °C under the applied voltage of 1.6 V. These resistivity values are higher than the minimum threshold (10^4 Ω cm) required for the sealants to work effectively in the SOEC conditions, in order to ensure the electrical insulation between two conductive Crofer22APU plates [30].

The electrical resistivity is comparable or even higher than the

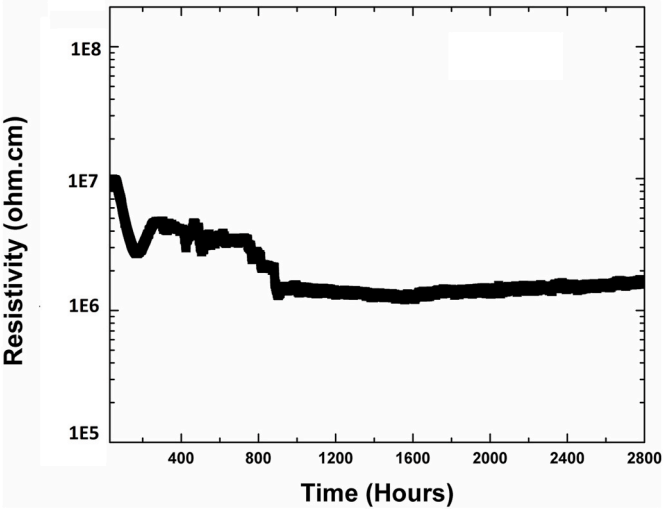

Fig. 2. Electrical resistivity of Crofer22APU/glass-ceramics/Crofer22APU joined samples for HJ4 glass-ceramics. These measurements were carried out at 850 °C with 1.6 V applied.

resistivity values reported in literature [28,29]. In reviewing the literature, Chou et al. [28] measured the electrical resistivity of a Crofer22APU/glass-ceramic/Crofer22APU joint in dual atmosphere. The Sr-based glass-ceramic showed the electrical resistivity in the range of 10^4-10^5 Ω cm as measured at 850 °C under the applied voltage of 0.7 V for 500 h. Similarly, in another study by Ghosh et al. [27], also reported the electrical resistivity of-10^6 Ω cm as measured for the series of glass-ceramics at 800 °C for 100 h.

From the graph above we can see that the electrical resistivity initially reduced up to 200 h followed by a constant behaviour up to 800 h. Around 800 h, some discontinuity was again observed and the resistivity values showed a reduction, followed by a steady constant behaviour till the end of test. The initial gradual reduction up to 200 h is most likely due to the presence of different free ions (such as Sr, Al and O), as HJ4 glass-ceramic has significantly high residual glassy phase after joining [34]. The free ions in the residual glassy phase can move under the high applied voltage of 1.6 V and testing temperature of 850 °C, therefore consequently reduce the resistivity. The second discontinuous behaviour observed after 800 h can be due to polarization effect. However, after 800 h the resistivity values for HJ4 based joint became constant until the end of test (2800 h). Further information and experimental evidence about interfacial phenomena can be deduced from SEM investigations of cross sections of Crofer22APU-HJ4 joined samples.

3.2. SEM post mortem analysis

Fig. 3 shows the SEM image of the anodic polarized Crofer22APU/HJ4 glass-ceramic interface after the electrical resistivity test in static air. The microstructure of the HJ4 glass-ceramic is homogenous, dense with slight presence of porosity and strong bonding and compatibility with the Crofer22APU substrate. The long term (2800 h) thermal ageing also resulted in the formation of an oxide scale at Crofer22APU/HJ4 glass-ceramic interface.

A bright crystalline phase is distributed within the residual amorphous matrix together with the presence of black crystals. The SEM analysis in backscattered mode resulted in different colour of phases depending upon their densities. The EDS point analyses were performed at different regions of HJ4 glass-ceramic after the electrical resistivity test. These regions are marked in Fig. 3 and their corresponding EDS analyses are given in Table 1. The EDS analyses carried out at point 1 shows that it corresponds to $SrSiO_3$ phase, similar to one observed in the HJ4 glass-ceramic after joining and after thermal ageing for 1000 h, as discussed in previous studies [14]. The EDS analyses performed at point 2 (black phase) confirmed the presence of cristobalite (SiO_2) phase (α-variant, which is stable at room temperature [36]). A small concentration (3.1 at %) of aluminium was also detected at point 2, however,

Table 1
EDS point analyses (at.%) performed on HJ4 glass-ceramic shown in Fig. 3, after electrical resistivity test for 2800 h in static air.

	Point 1	Point 2	Point 3
O	71.2	75.6	73.4
Si	21.5	21.3	16.2
Sr	7.2	–	7.4
Al	–	3.1	2.0
Y	–	–	0.7

the morphology of black phase (point 2) is similar to cristobalite phase observed in previous studies, and referred as low temperature cristobalite [37]. Even if cristobalite is considered potentially dangerous for the integrity of the sealants (due to its volume change around 230–270 °C [38]) its presence in the microstructure of the glass-ceramic is limited and no presence of cracks starting from cristobalite particles was detected. Point 3 in Fig. 3 corresponds to the residual glassy phase. The residual glassy phase contains 7.4 at % of Sr, which is beneficial to maintain viscous behaviour of residual glass. The SEM image (Fig. 3) also shows that even after thermal ageing of 2800 h at 850 °C, a significant residual glass is still present. This residual glass can promote the self-healing and thermal stress mitigation, above the glass transition temperature (T_g).

Fig. 4 shows the EDS mapping of the anodic polarized Crofer22APU/HJ4 glass-ceramic interface after the resistivity test. A thin (≈ 2 μm) Cr rich oxide scale is present on the surface of Crofer22APU; however, Cr is confined within the oxide scale without any diffusion into the HJ4 glass-ceramic side was found. However, some traces of Mn diffusion into the residual glass are observed. Besides that, no other element of glass-ceramic diffused or segregate at interface with Crofer22APU. These results also confirmed that HJ4 glass-ceramic is chemically stable after high temperature and long term ageing under electric load.

The formation of $SrCrO_4$ is commonly observed in Sr-based glasses and can adversely affect the compatibility of sealants with Cr-based metallic interconnects [39]. However, even in the presence Cr-rich oxide scale, the Crofer22APU/sealant interface did not show any evidence of $SrCrO_4$ phase, thus ensuring a stable adhesion and bonding.

The SEM post mortem analysis of the cathodic polarized Crofer22APU/HJ4 glass-ceramic interface after the resistivity test is shown in Fig. 5, while the corresponding EDS analyses carried out at the HJ4 glass-ceramic are given in Table 2. A uniform and dense microstructure of HJ4 glass-ceramic is evident from the SEM post mortem analyses. The EDS point analyses confirmed the presence of the $SrSiO_3$ (point 1) and cristobalite (point 2) phases in addition to the residual glassy phase (point 3). From the EDS point analysis, no Cr diffusion was detected from Crofer22APU substrate into the glass-ceramic side.

Likewise, anodic polarized Crofer22APU/HJ4 glass-ceramic

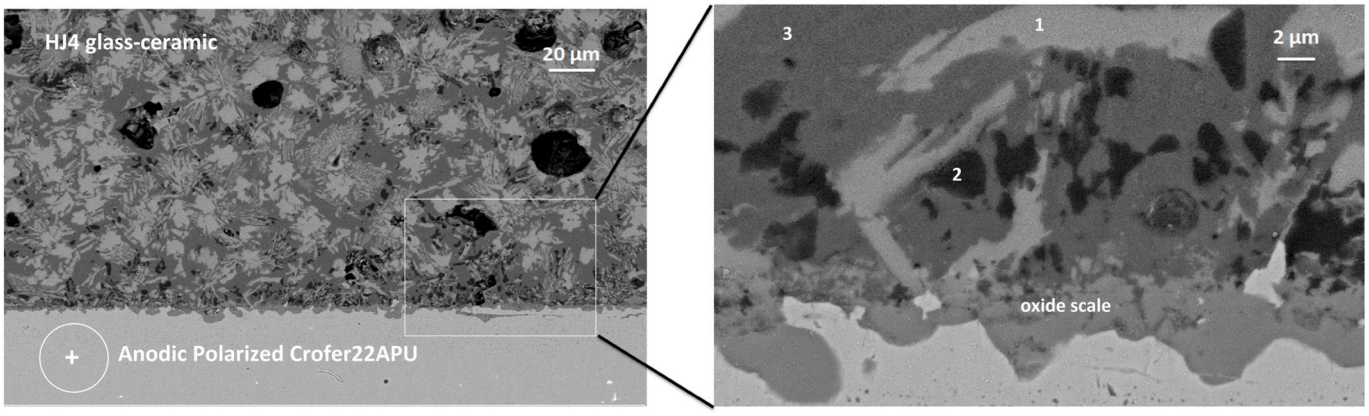

Fig. 3. Post mortem SEM image of the anodic polarized Crofer22APU/HJ4 glass-ceramic interface, after the electrical resistivity test for 2800 h in static air, under a voltage of 1.6 V.

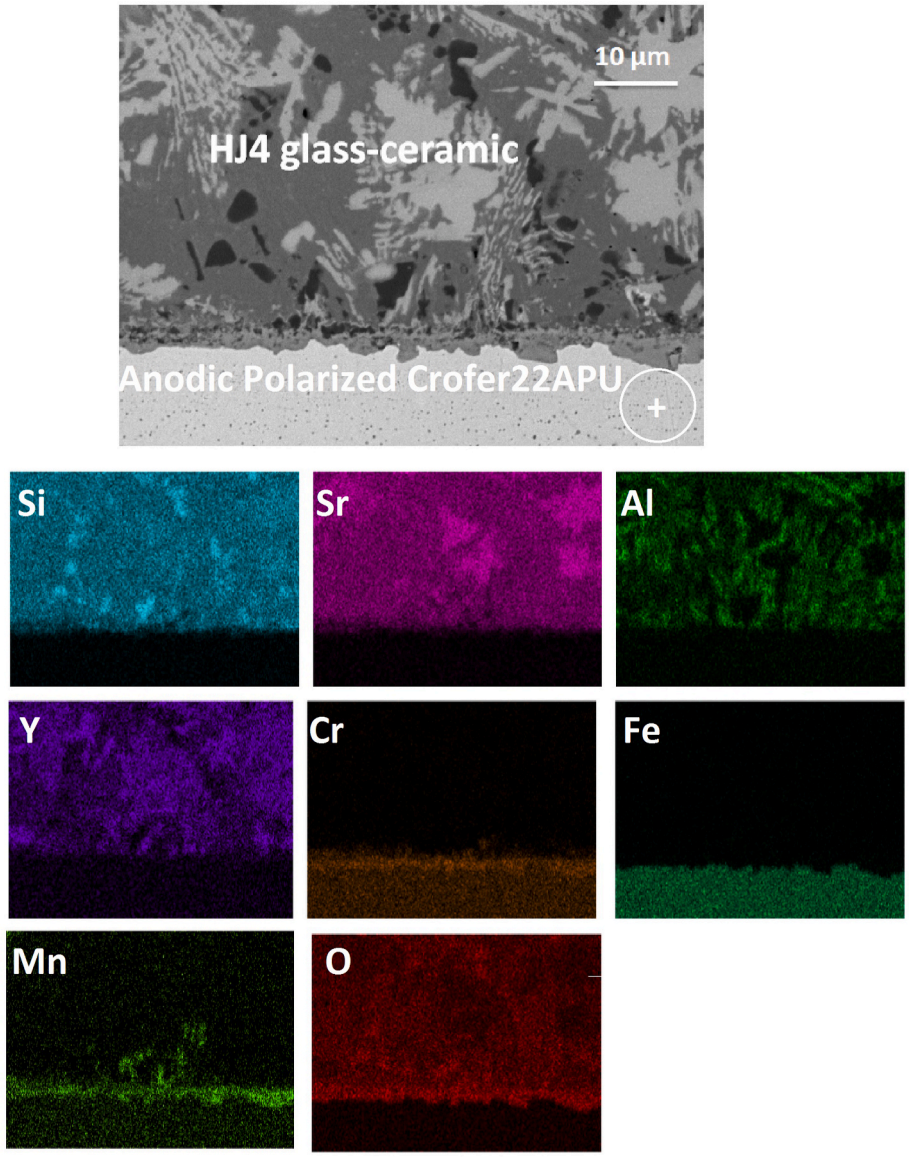

Fig. 4. EDS mapping of the SEM image corresponding to the post mortem analyses of anodic polarized Crofer22APU/HJ4 glass-ceramic interface, after the electrical resistivity test for 2800 h in static air, under a voltage of 1.6 V

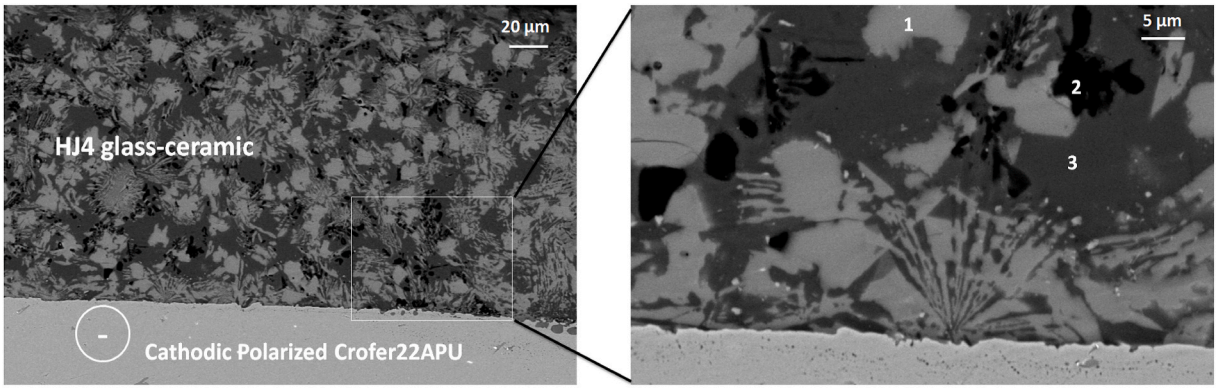

Fig. 5. Post mortem SEM image of cathodic polarized Crofer22APU/HJ4 glass-ceramic interface, after the electrical resistivity test for 2800 h in static air, under a voltage of 1.6 V

Table 2
EDS point analyses (at.%) performed on HJ4 glass-ceramic shown in Fig. 5, after electrical resistivity test for 2800 h in static air.

	Point 1	Point 2	Point 3
O	57.6	65.1	67.1
Si	23.0	34.9	20.1
Sr	19.4	–	9.3
Al	–	–	3.2
Y	–	–	0.3

interface, no segregation of glass-ceramic components within glass or at Crofer22APU/sealant interface was detected in case of cathodic polarized Crofer22APU/HJ4 glass-ceramic interface. On the other hand, the EDS mapping (Fig. 6) indicates that a small concentration of Cr and Mn has been diffused from the Crofer22APU interconnect towards the HJ4 glass-ceramic side. Furthermore, the oxide scale appears to be thinner and more irregular on the cathodic interface than on the anodic one. A similar behaviour was pointed out by Sabato et al. [32] where outward diffusion of Cr and Mn was recorded in proximity of the cathodic polarized interface. In that case, ≈ 4 at.% Cr was detected at 6-10 μm from the interface (after 100 h of test). The diffusion in this work is much more limited, due to lower presence of amorphous phase which represents a preferred path for diffusion of Cr ions at high temperature. Nevertheless, no chemical interaction or traces of formation of $SrCrO_4$ phase were found from SEM-EDS analyses, thus confirming an excellent compatibility with the Crofer22APU substrate.

3.3. XRD analysis

The XRD analysis on HJ4 sample after heat-treatment at 850 °C for 2800 h is shown in Fig. 7. The XRD peaks correspond to the $SrSiO_3$ as the main crystalline phase; in addition to cristobalite (SiO_2) as secondary phase, similar to the as joined HJ4 glass-ceramic, as reported in previous studies [14]. A peak at $2\Theta = 28.8°$ is doubtful and unidentified due to the complex microstructure of the glass ceramic, as it was already pointed out in a previous work [34]. It must be noted that the indexing of the peaks at $2\Theta = 27.5°$ and 27.8° is still uncertain and ambiguous; these peaks might be attributed to the $SrAlSi_2O_8$ (Reference code: 01-70-1862) feldspar strontian-monocelsian (stable at RT), but 3rd and 4th (for intensity) peaks at $2\Theta = 25.97°$ and 35.17° are not present in the diffraction pattern of HJ4 glass-ceramic. Anyway, EDS maps excluded the formation of $SrAlSi_2O_8$. Therefore, the presence of the monoclinic

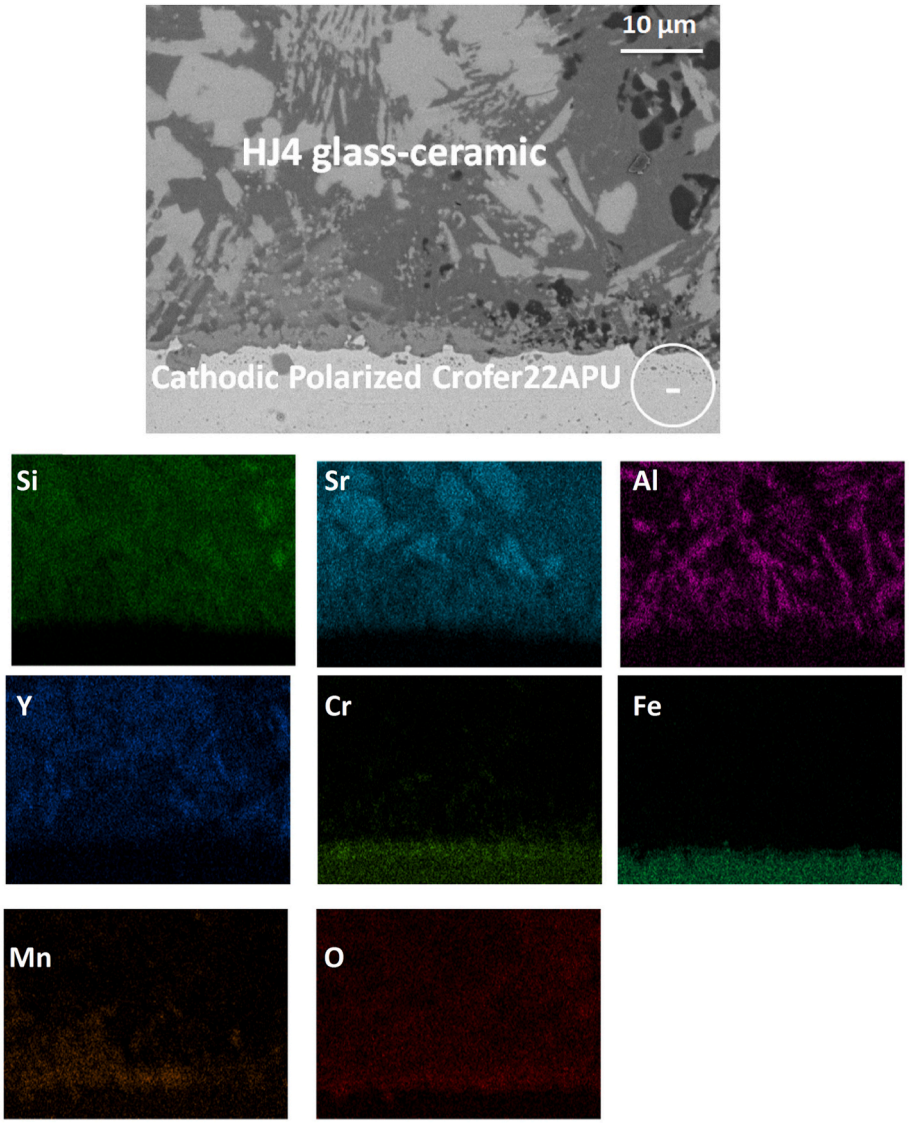

Fig. 6. EDS mapping of SEM image corresponding to post mortem analyses of cathodic polarized Crofer22APU/HJ4 glass-ceramic interface, after the electrical resistivity test for 2800 h in static air, under a voltage of 1.6 V

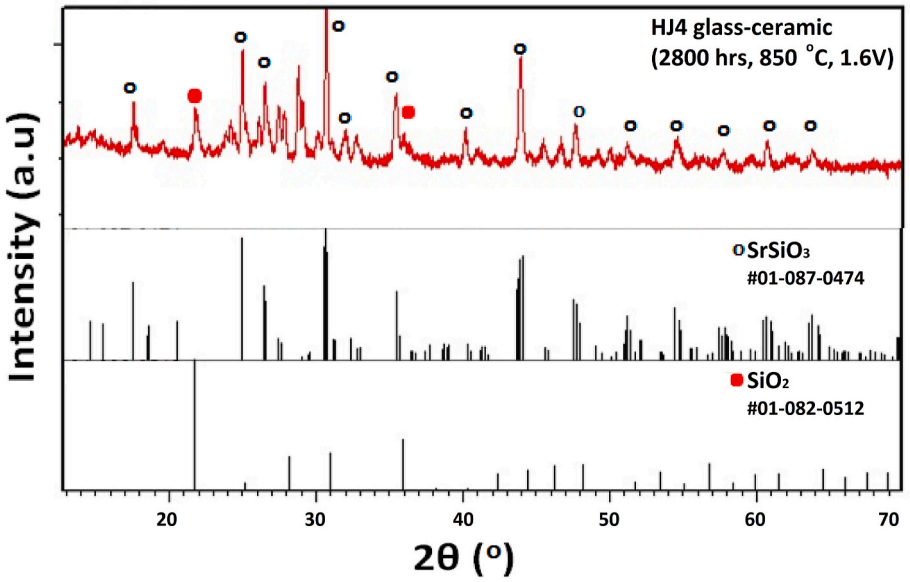

Fig. 7. XRD of HJ4 glass-ceramic after electrical resistivity test in static air (2800 h, 850 °C, 1.6 VV).

$SrAlSi_2O_8$ should be carefully evaluated in future work.

As mentioned in the literature review, few studies reported and discussed the electrical resistivity of sealants-interconnects in harsh conditions. Even if a large and growing body of literature has investigated SrO containing glasses [40–42], most of these papers have focused on the temperature dependence of electrical conductivity for glasses and sintered glass-ceramics not in contact with metallic interconnects (at 750 °C for 1000 h and the conductivity of glass-ceramics at 750 °C as a function of heat-treatment time) or on tuning the interfacial reaction between SrO-bases glass and Crofer22APU [43]. Qi Zhang et al. [44] studied the effect of Nb_2O_5 doping on improving the thermo-mechanical stability of Sr-containing glass sealing, but the temperature dependence of conductivity is reported without considering the effect of applied voltage on possible interfacial reactions affecting the electrical measurements.

Our study has shown and discussed the influence on microstructure and composition of a previously designed glass-ceramic sealant for SOEC application. These findings have important implications for developing reliable glass-ceramic sealants SOECs. The results presented in this paper are significant in at least two major respects:

- The stability of electrical resistance of Crofer22APU/glass-ceramic/Crofer22APU joined samples was evaluated in a long term test at 850 °C.
- Experimental evidence excluded the presence of detrimental reactions (such as Sr-chromates) or new phases formation at the Crofer22APU/glass-ceramic sealants (both anodic and cathodic polarized) interfaces, when triggered by the relatively high applied potential (1.6 V).

4. Conclusions

Crofer22APU/glass-ceramic sealant/Crofer22APU joined samples showed electrical resistivity in the range of 10^6-10^7 Ω cm, sufficiently high to ensure insulation for solid oxide electrolysis cell application. The SEM-EDS post mortem analysis showed a uniform microstructure after electrical resistivity analysis for 2800 h at 850 C under the applied voltage of 1.6 V. No evidence of diffusion of elements across Crofer22APU/glass-ceramics interface was observed, thus confirming the good stability of the proposed glass-ceramic sealant under SOEC harsh conditions and possible detrimental interfacial reactions triggered by 1.6 V applied.

Declaration of competing interest

The authors declare that they have no known competing financial interests or personal relationships that could have appeared to influence the work reported in this paper.

Acknowledgements

The research leading to this work received funding from:(a) European Commission's Fuel Cells Hydrogen Joint Undertaking (FCH 2 JU), grant agreement No 874577 – NewSOC.(b) The European Union's Horizon 2020 research and innovation programme under the Marie Sklodowska-Curie grant agreement No 642557 (CoACH-ETN).

References

[1] W. Dönitz, E. Erdle, High-temperature electrolysis of water vapor-status of development and perspectives for application, Int. J. Hydrogen Energy 10 (1985) 291–295, https://doi.org/10.1016/0360-3199(85)90181-8.
[2] Q. Li, Y. Zheng, W. Guan, L. Jin, C. Xu, W.G. Wang, Achieving high-efficiency hydrogen production using planar solid-oxide electrolysis stacks, Int. J. Hydrogen Energy 39 (2014) 10833–10842, https://doi.org/10.1016/j.ijhydene.2014.05.070.
[3] a. Hauch, S.D. Ebbesen, S.H. Jensen, M. Mogensen, Solid oxide electrolysis cells: microstructure and degradation of the Ni/Yttria-Stabilized zirconia electrode, J. Electrochem. Soc. 155 (2008) B1184, https://doi.org/10.1149/1.2967331.
[4] A. Pandiyan, A. Uthayakumar, R. Subrayan, S.W. Cha, S.B. Krishna Moorthy, Review of solid oxide electrolysis cells: a clean energy strategy for hydrogen generation, Nanomater. Energy 8 (2019) 2–22, https://doi.org/10.1680/jnaen.18.00009.
[5] D. Ferrero, A. Lanzini, M. Santarelli, P. Leone, A comparative assessment on hydrogen production from low- and high-temperature electrolysis, Int. J. Hydrogen Energy 38 (2013) 3523–3536, https://doi.org/10.1016/j.ijhydene.2013.01.065.
[6] H. Khedim, H. Nonnet, F.O. Méar, Development and characterization of glass-ceramic sealants in the (CaO-Al 2O 3-SiO 2-B 2O 3) system for solid oxide electrolyzer cells, J. Power Sources 216 (2012) 227–236, https://doi.org/10.1016/j.jpowsour.2012.05.041.
[7] H. Elsayed, H. Javed, A.G. Sabato, F. Smeacetto, E. Bernardo, Novel glass-ceramic SOFC sealants from glass powders and a reactive silicone binder, J. Eur. Ceram. Soc. 38 (2018) 4245–4251, https://doi.org/10.1016/j.jeurceramsoc.2018.05.024.
[8] H. Javed, A.G. Sabato, M. Mansourkiaei, D. Ferrero, M. Santarelli, K. Herbrig, C. Walter, F. Smeacetto, Glass-ceramic sealants for SOEC : thermal characterization and electrical resistivity in dual atmosphere, Energies 13 (2020) 3682, https://doi.org/10.3390/en13143682.
[9] M. Palcut, L. Mikkelsen, K. Neufeld, M. Chen, R. Knibbe, P.V. Hendriksen, Corrosion stability of ferritic stainless steels for solid oxide electrolyser cell interconnects, Corrosion Sci. 52 (2010) 3309–3320, https://doi.org/10.1016/j.corsci.2010.06.006.
[10] J. Wu, X. Liu, Recent development of SOFC metallic interconnect, J. Mater. Sci. Technol. 26 (2010) 293–305, https://doi.org/10.1016/S1005-0302(10)60049-7.

[11] J. Puig, A. Prange, B. Arati, C. Laime, P. Lenormand, F. Ansart, Optimization of the synthesis route of a barium boron aluminosilicate sealing glass for SOFC applications, Ceram. Int. (2017) 1–6, https://doi.org/10.1016/j.ceramint.2017.04.151.
[12] G. Kaur, Solid Oxide Fuel Cell Components: Seal Glass for Solid Oxide Fuel Cells, 2006, https://doi.org/10.1007/s11837-006-0052-6.
[13] M. Fakouri Hasanabadi, M.A. Faghihi-Sani, A.H. Kokabi, S.M. Groß-Barsnick, J. Malzbender, Room- and high-temperature flexural strength of a stable solid oxide fuel/electrolysis cell sealing material, Ceram. Int. (2018), https://doi.org/10.1016/j.ceramint.2018.09.236.
[14] H. Javed, A.G. Sabato, K. Herbrig, D. Ferrero, C. Walter, M. Salvo, F. Smeacetto, Design and characterization of novel glass-ceramic sealants for solid oxide electrolysis cell (SOEC) applications, Int. J. Appl. Ceram. Technol. 15 (2018) 999–1010, https://doi.org/10.1111/ijac.12889.
[15] I. Ritucci, K. Agersted, P. Zielke, A.C. Wulff, P. Khajavi, F. Smeacetto, A.G. Sabato, R. Kiebach, A Ba-free sealing glass with a high coefficient of thermal expansion and excellent interface stability optimized for SOFC/SOEC stack applications, Int. J. Appl. Ceram. Technol. 15 (2018) 1011–1022, https://doi.org/10.1111/ijac.12853.
[16] H. Lee, U.S. Kim, S.D. Kim, S.K. Woo, W.J. Chung, SiO2–B2O3-BaO-WO3 glasses with varying Al2O3 content as a sealing material for reversible solid oxide fuel cells, Ceram. Int. 46 (2020) 18256–18261, https://doi.org/10.1016/j.ceramint.2020.04.148.
[17] M. Ferraris, S. De la Pierre, A.G. Sabato, F. Smeacetto, H. Javed, C. Walter, J. Malzbender, Torsional shear strength behavior of advanced glass-ceramic sealants for SOFC/SOEC applications, J. Eur. Ceram. Soc. 40 (2020) 4067–4075, https://doi.org/10.1016/j.jeurceramsoc.2020.04.034.
[18] T. Osipova, J. Wei, G. Pecanac, J. Malzbender, Room and elevated temperature shear strength of sealants for solid oxide fuel cells, Ceram. Int. 42 (2016) 12932–12936, https://doi.org/10.1016/j.ceramint.2016.05.064.
[19] S. Wang, Y. Wang, Y. Hsu, C. Chuang, Effect of additives on the thermal properties and sealing oxide fuel cell application, Int. J. Hydrogen Energy 34 (2009) 8235–8244, https://doi.org/10.1016/j.ijhydene.2009.07.094.
[20] M.K. Mahapatra, K. Lu, Seal glass for solid oxide fuel cells, J. Power Sources 195 (2010) 7129–7139, https://doi.org/10.1016/j.jpowsour.2010.06.003.
[21] F. Smeacetto, A. Chrysanthou, M. Salvo, T. Moskalewicz, F. D'Herin Bytner, L. C. Ajitdoss, M. Ferraris, Thermal cycling and ageing of a glass-ceramic sealant for planar SOFCs, Int. J. Hydrogen Energy 36 (2011) 11895–11903, https://doi.org/10.1016/j.ijhydene.2011.04.083.
[22] A.G. Sabato, G. Cempura, D. Montinaro, A. Chrysanthou, M. Salvo, E. Bernardo, M. Secco, F. Smeacetto, Glass-ceramic sealant for solid oxide fuel cells application: characterization and performance in dual atmosphere, J. Power Sources 328 (2016) 262–270, https://doi.org/10.1016/j.jpowsour.2016.08.010.
[23] Z. Luo, W. Lei, H. Liang, W. Xu, X. Liu, C. Qin, A. Lu, Improving sealing properties of CaO-SrO-Al2O3-SiO2 glass and glass-ceramics for solid oxide fuel cells: effect of La2O3 addition, Ceram. Int. 46 (2020) 17698–17706, https://doi.org/10.1016/j.ceramint.2020.04.074.
[24] R. Li, X. Liang, X. Wang, W. Zeng, J. Yang, D. Yan, J. Pu, B. Chi, J. Li, Improvement of sealing performance for Al2O3 fiber-reinforced compressive seals for intermediate temperature solid oxide fuel cell, Ceram. Int. 45 (2019) 21953–21959, https://doi.org/10.1016/j.ceramint.2019.07.209.
[25] M.S. Domenico Ferrero, Andrea Lanzini, Pierluigi Leone, Dynamic reversible SOC applications: performance and Durability with simulated load/demand profiles, in: Proceedings of 11th European SOFC and SOE Forum 2014 : Chapter 17 - Session B14. SOE Systems, European Fuel Cell Forum, 2014, pp. 60–67.
[26] P. Batfalsky, V.A.C. Haanappel, J. Malzbender, N.H. Menzler, V. Shemet, I. C. Vinke, R.W. Steinbrech, Chemical interaction between glass-ceramic sealants and interconnect steels in SOFC stacks, J. Power Sources 155 (2006) 128–137, https://doi.org/10.1016/j.jpowsour.2005.05.046.
[27] S. Ghosh, A. Das Sharma, P. Kundu, R.N. Basu, Glass-ceramic sealants for planar IT-SOFC: a bilayered approach for joining electrolyte and metallic interconnect, J. Electrochem. Soc. 155 (2008) B473–B478, https://doi.org/10.1149/1.2883732.
[28] Y.S. Chou, J.W. Stevenson, G.G. Xia, Z.G. Yang, Electrical stability of a novel sealing glass with (Mn,Co)-spinel coated Crofer22APU in a simulated SOFC dual environment, J. Power Sources 195 (2010) 5666–5673, https://doi.org/10.1016/j.jpowsour.2010.03.052.
[29] Q. Zhu, L. Peng, T. Zhang, Y.-S.S. Chou, J.W. Stevenson, J.-P. Choi, K.D. Meinhardt, Alkali effect on the electrical stability of a solid oxide fuel cell sealing glass, Fuel Cell Electronics Packaging 93 (2010) 618–623, https://doi.org/10.1111/j.1551-2916.2009.03466.x.
[30] S. Ghosh, A. Das Sharma, P. Kundu, R.N. Basu, Glass-based sealants for application in planar solid oxide fuel cell stack, Trans. Indian Ceram. Soc. 67 (2008) 161–182, https://doi.org/10.1080/0371750X.2008.11078652.
[31] A. Rost, J. Schilm, M. Kusnezoff, A. Michaelis, Degradation of sealing glasses under electrical load, European Fuel Cell Forum 80 (2010) 1–12, https://doi.org/10.4416/JCST2012-00002.
[32] A.G. Sabato, A. Rost, J. Schilm, M. Kusnezoff, M. Salvo, A. Chrysanthou, F. Smeacetto, Effect of electric load and dual atmosphere on the properties of an alkali containing diopside-based glass sealant for solid oxide cells, J. Power Sources 415 (2019) 15–24, https://doi.org/10.1016/J.JPOWSOUR.2019.01.051.
[33] S. Ghosh, A. Das Sharma, P. Kundu, S. Mahanty, R.N. Basu, Development and characterizations of BaO-CaO-Al2O3-SiO2 glass-ceramic sealants for intermediate temperature solid oxide fuel cell application, J. Non-Cryst. Solids 354 (2008) 4081–4088, https://doi.org/10.1016/j.jnoncrysol.2008.05.036.
[34] H. Javed, A.G. Sabato, I. Dlouhy, M. Halasova, E. Bernardo, M. Salvo, K. Herbrig, C. Walter, F. Smeacetto, Shear performance at room and high temperatures of glass–ceramic sealants for solid oxide electrolysis cell technology, Materials 12 (2019) 298, https://doi.org/10.3390/ma12020298.
[35] X. Wang, D.R. Ou, Z. Zhao, M. Cheng, Stability of SrO–La2O3–Al2O3–SiO2 glass sealants in high-temperature air and steam, Ceram. Int. 42 (2016) 7514–7523, https://doi.org/10.1016/j.ceramint.2016.01.158.
[36] S. Dai, M.A. Rodriguez, J.J.M. Griego, W.C. Wei, Sealing glass-ceramics with near linear thermal strain, Part I: process development and phase identification, J. Am. Ceram. Soc. 99 (2016) 3719–3725, https://doi.org/10.1111/jace.14364.
[37] J. Schilm, A. Rost, M. Kusnezoff, S. Megel, A. Michaelis, Glass ceramics sealants for SOFC interconnects based on a high chromium sinter alloy, Int. J. Appl. Ceram. Technol. 15 (2018) 239–254, https://doi.org/10.1111/ijac.12811.
[38] M.D. Beals, S. Zerfoss, Volume change attending low-to-high inversion of cristobalite, J. Am. Ceram. Soc. 27 (1944) 285–292, https://doi.org/10.1111/j.1151-2916.1944.tb14471.x.
[39] Y.S. Chou, J.W. Stevenson, P. Singh, Effect of pre-oxidation and environmental aging on the seal strength of a novel high-temperature solid oxide fuel cell (SOFC) sealing glass with metallic interconnect, J. Power Sources 184 (2008) 238–244, https://doi.org/10.1016/j.jpowsour.2008.06.020.
[40] H. Liu, X. Du, Z. Yu, D. Tang, T. Zhang, The phase evolution, electrical stability and chemical compatibility of sealing glass-ceramics for solid oxide fuel cell applications: effect of La2O3 or CeO2, RSC Adv. 6 (2016) 17151–17157, https://doi.org/10.1039/c5ra23357g.
[41] Q. Zhang, H. Yang, F. Zeng, S. Wang, D. Tang, T. Zhang, Development of the CaO – SrO – ZrO2 – B2O3 – SiO2 sealing glasses for solid oxide fuel cell Applications : structure, RSC Adv. 5 (2015) 41772–41779, https://doi.org/10.1039/C5RA04781A.
[42] P.K. Ojha, T.K. Chongdar, N.M. Gokhale, A.R. Kulkarni, Investigation of crystallization kinetic of SrO-La2O3-Al2O3-B2O3-SiO2 glass and its suitability for SOFC sealant, Int. J. Hydrogen Energy 36 (2011) 14996–15001, https://doi.org/10.1016/j.ijhydene.2010.12.120.
[43] Q. Zhang, L. Fang, J. Shen, M.J. Pascual, T. Zhang, Tuning the interfacial reaction between bismuth-containing sealing glasses and Cr-containing interconnect: effect of ZnO, J. Am. Ceram. Soc. 98 (2015) 3797–3806, https://doi.org/10.1111/jace.13779.
[44] Q. Zhang, X. Du, S. Tan, D. Tang, K. Chen, T. Zhang, Effect of Nb 2 O 5 doping on improving the thermo-mechanical stability of sealing interfaces for solid oxide fuel cells, 2017, pp. 1–8, https://doi.org/10.1038/s41598-017-05725-y.